https://dx.doi.org/10.4314/gjgs.v17i1.5

GLOBAL JOURNAL OF GEOLOGICAL SCIENCES VOL. 16, 2018: 53-60
COPYRIGHT© BACHUDO SCIENCE CO. LTD PRINTED IN NIGERIA ISSN 1596-6798
www.globaljournalseries.com, Email: info@globaljournalseries.com

SUBSURFACE ELECTRICAL RESISTIVITY IMAGING AND ELECTROMAGNETIC CONDUCTIVITY PROFILING AT A PROPOSED CONSTRUCTION SITE AT ADEKUNLE AJASIN UNIVERSITY CAMPUS, AKUNGBA-AKOKO, SOUTH-WESTERN NIGERIA

MUSLIM B. AMINU

(Received 25 September 2018; Revision Accepted 9 November 2018)

ABSTRACT

Electrical resistivity imaging and co-planar loop electromagnetic conductivity measurements have been employed to delineate the bedrock topography and subsurface distribution of structural features at a construction site on the campus of Adekunle Ajasin University. The goal was to map the subsurface geological disposition and to identify features which could adversely impact on the ongoing construction works. Data were collected along three geophysical traverses using the ABEM1000 Terrameter unit and the EM34 Co-planar loop electromagnetic system. Traverse 1 trend roughly east-west for a total length of 155m while traverses 2 and 3 are trend north-south for 80m each. The collection of electrical resistivity data utilized the dipole-dipole array with an electrode separation of 5 m and maximum dipole spread of 35m. Observed field data were processed and inverted using a finite-element modelling inversion algorithm. Conductivity were collected at 10m coil separation and plotted against station positions. A station separation of 5m was maintained on all traverses for both data sets. Three geo-electric layers were delineated; a thin highly discontinuous low resistivity layer representing the humus-rich top soil, a continuous consistently high resistivity layer with a highly rugose upper layer and several near vertical scarps representing the fresh bedrock and intermediate resistivity layer representing the weathered bedrock separating the upper low resistivity and basal high resistivity signatures. Overburden thickness rarely exceeds 4 m with the exception of the deep weathering section in the southwest and at fracture points with the bedrock. Perennial groundwater flow at the site is restricted to the south-eastern sections of the site.

KEYWORDS: Akungba-Akoko, electrical resistivity imaging, ground conductivity, bedrock structure, foundation studies.

1. INTRODUCTION

Non-invasive geophysical techniques offer rapid and cost effective screening of subsurface geologic structure for mineral exploration, groundwater prospecting, and environmental and engineering investigations (Zume et al., 2006; Frid et al., 2007; Lines et al., 2012, Mohamed et al., 2012; Moustafa et al., 2012). In construction site investigations, they offer semi-continuous and sometimes continuous profiling of structures inimical to civil works projects (Soupios et al., 2002; El-Qady et al., 2005; Chavez et al., 2014; Yassin et al., 2014). They also provided information on the thickness of the regolith and depth to competent bedrock or formations (Robineau et al., 2007), morphology and spatial distribution of underlying geo-features (Aminu, 2015a), groundwater regimes (Rizzo et al., 2004; Bufford et al., 2012; Aminu et al., 2014) and ground corrosivity (). They sometimes provide quantitative estimates of insitu geo-technical properties (Anderson, 2006; Cosenza et al., 2006) of the subsurface geologic strata and clues to the tectonic history of surveyed areas (Bufford et al., 2012; Aminu et al., 2014). They therefore present some advantages over conventional geotechnical methods which are generally more expensive, time consuming and often (as a result of prohibitive cost) sparsely sample the subsurface. For these reasons, geophysical methods have found considerable applications in civil works site investigation. This progression has been encouraged by the development of newer techniques, computing power and algorithms to invert several geophysical data types for images of the subsurface and estimation of subsurface parameters (Loke 2000). The most commonly applied geophysical methods are the class of electrical methods, those employing electrical resistivity or electrical conductivity. The attraction lies in the relative ease of implementation, robustness of the inversion results and the spatial imaging in 2 and 3 dimensions obtainable for the methods (Bufford et al., 2012; Robineau et al., 2007).

In this study, the site of an ongoing Faculty building on Adekunle Ajasin University Campus was investigated using a combination of 2D electrical

Muslim B. Aminu, Department of Earth Sciences, Adekunle Ajasin University, Akungba-Akoko, Nigeria.

resistivity imaging and co-planar loop electromagnetic conductivity data. This way, insight was gained into the subsurface geologic disposition and possible ground water pathways at the site.

Prior, Aminu (2015a; 2015b), had utilized 2D electrical resistivity imaging to delineate subsurface structure favourable to ground water storage and those inimical to construction works on the university campus. The major takeaways from these earlier studies are the conclusions that the subsurface on the university campus usually presented with a thin overburden and highly rugose bedrock topography. The fresh bedrock outcrops at short intervals and deep weathering sections and fracture systems often segment the fresh bedrock rock and act at subsurface conduits for the accumulation and migration of groundwater.

2. Site of Investigation

The University campus lies in the north of Akungba Township towards the north-eastern end of Ondo State, Nigeria (figure, 1). Akungba is situated between Longitudes 05˚ 43' and 05 ˚ 47', and Latitudes 07˚ 27' and 07˚ 31'. Physiographically, the area consists of a southward sloping and central low lying area surrounded in a perimeter-like fashion by high rising granitic hills to the north, west and southeast. Topography rises in excess of 345 m above sea-level and reaches up to 420 m above sea-level at the summits of the northern granitic ridges. Lithologically, the area is underlain by migmatite-gneiss complexes of the basement rocks of the south-western Nigeria (Rahaman, 1989). Dominant rocks include biotite-rich grey gneiss, granite gneiss and minor occurrences of charnockitic rocks. Drainage is provided by a number of seasonal streams which take their source from high reliefs in the northeast. Over burden thicknesses are low and fresh basement rocks frequently outcrop at short intervals in several parts of the area. Rocks in the area have suffered multiple episodes of tectonic deformations. This has given rise to an abundance of deformation structures including folds and fractures. Drainage courses are to a large extent controlled by major and persistent frequently open-to-surface fracture paths.

The survey site is in the western section of the Adekunle Ajasin University campus (figure 1). The site is relatively flat and is located on the northern side of a major east-west University road. It covers an area of approximately 1.7km^2. Foundation works of the proposed faculty of sciences building have been concluded. Approximately 40 m west of the foundation structure, a slight depression accommodates a seasonal streamlet which runs in the north-south direction. To the north and northeast of the complex, basement rocks are seen to outcrop. Surface cover consists of humus-rich sandy loams which generally appear well drained.

3. Methodology

Data Collection

Three (3) traverses were surveyed in the study area. Traverse 1 (Tr. 1) spanned a total length of 155 m. It runs roughly in the west to east direction, approximately 15 m from the southern perimeter of the foundation wall structure of the proposed Science building. Traverse 2 (Tr. 2) and Traverse 3 (Tr. 3) run from south to north, each 10 m from the western and eastern ends of the building respectively. Both traverses were 80 m in length. Spatial relationships between the traverses are captured graphically in figure 1. Data collected included 2D Electrical resistivity and co-planar loop electrical conductivity data. The electrical resistivity data were collected using the ABEM 1000 Terrameter system. The dipole-dipole electrode configuration was utilized in order to capture lateral as well as vertical variations in conditions of the subsurface. Dipole spacing on all traverses was 5 m and a maximum dipole length of 35 m was achieved all through the survey. Ground electrical conductivity data were collected at 5 m intervals along the traverses using the Geonics Co-planar loop EM34 system. A coil separation of 10 m was utilized. Data were collected in March, 2017, prior to the onset of seasonal rains.

Processing

Acquired resistivity data were processed and data inversion was carried out using a 2.5D finite element modelling inversion algorithm (DIPROfWIN 4.01) described in Yi and Kim, (1998). The program computes an initial model and then attempts to minimize the difference between it and the observed resistivity fields until a reasonable fit is achieved. The program output three images, the observed field data pseudo-section, the computed theoretical data pseudo-section and the inverted subsurface resistivity structure. Considering the wide range of inverted resistivity (15 – 7000 Ohm-m) a logarithmic colour display was utilized and display was limited to the range 90 – 5000 Ohm-m as these provided the best visual presentation of resistivity distributions along the traverses.

Interpretation Criteria

Interpretation criteria for resulting 2D subsurface resistivity structure of the subsurface followed similar criteria to that utilized in Aminu et al. (2014), Aminu (2015a) and Aminu (2015b). High laterally and or vertically continuous resistivities (usually above 1000 Ohm-m) were interpreted to indicate unfractured basement rock. Low continuous-in-the-subsurface resistivities (usually below 150 Ohm-m) were interpreted to represent water saturated surficial humus and clay-rich top-soil. Resistivities ranging from 160 – 900 Ohm-m were interpreted as partly weathered basement rocks and conductive fracture paths depending on the lateral and vertical continuity and geometry of the imaged responses.

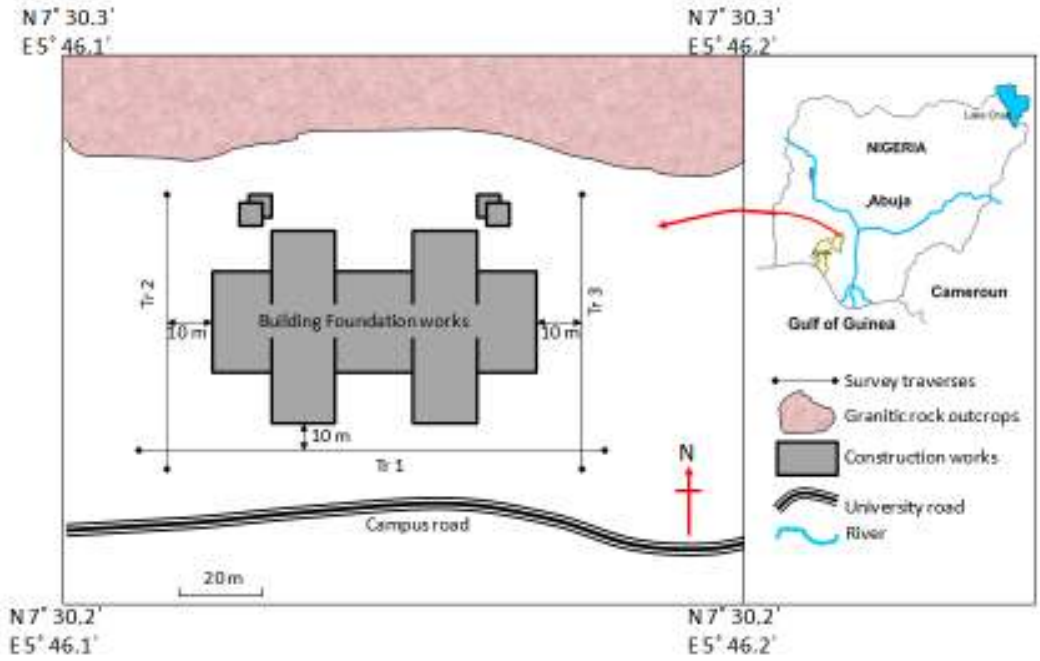

Figure. 1: Location map of the survey area. Survey traverses are indicated in solid black lines.Site is bounded to the north by granitic high which rise in excess of 80 m above the sourounding plains and to the south by ae east-west university road.

4. RESULTS

Electrical Resistivity

Figure 2 is a composite image consisting of the inverted subsurface 2D resistivity structure along Tr. 1 and the corresponding subsurface conductivity plot. The subsurface resistivity structure along Tr. 1 is characterized by three fairly distinct response patterns. The first pattern consists of multiple pockets of discontinuous very low resistivity responses with resistivities generally less than 150 Ohm-m. This pattern occurs at the surface at the locations 40 – 60 m, 78 – 84 m, 97 – 115 m and 135 – 147 m. This pattern rarely extends beyond a depth of 4 m below the surface with the exception of the location 125 – 133 m where it extends from a depth of approximately 1.5 m to 7 m.

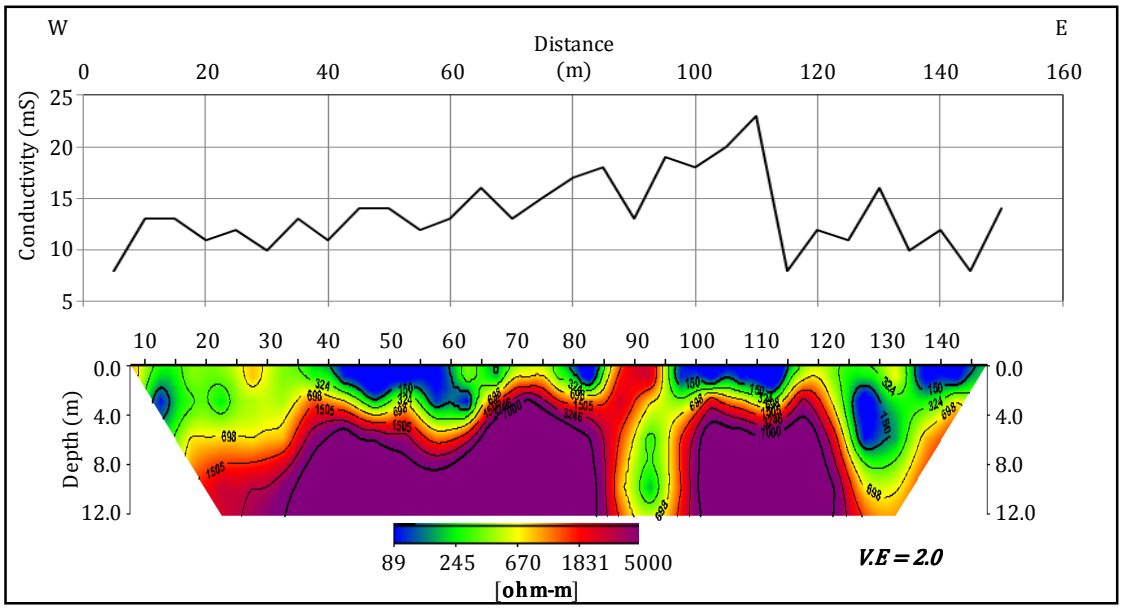

Figure. 2: Composite plot of inverted 2D subsurface resistivity structure (bottom) and ground conductivity at 10m coil separation (top) along traverse 1. Multiple bedrock highs with associate pinnacle troughs characterize the site. Troughs generally accommodate very low resistivity facies. Bedrock expressions often terminate in near-vertical edges which are coincident with measured high ground conductivity. (Vertical exaggeration in the 2D subsurface resistivity structure ≈ 2.0)

The second pattern consists of consistently high resistivity responses having resistivities generally in-excess of 1000 Ohm-m. Along the traverse, this response pattern is fairly continuous at depth extending from 15 - 124 m mark. It is segmented into western and eastern sections by a lower resistivity response pattern which extends between 87 m and 96 m. Its upper surface is highly rugose and extends from depths as shallow as 2 m below the ground surface. Between 38 – 68 m and 100 – 117 m, its upper surface forms two shallow troughs which accommodate the more extensive of the low resistivity responses described earlier. The lateral limits of this pattern are defined by near-vertical edges. The exception is the western end of the traverse where the pattern follows a high slope to a depth of 7 m between 40 m and 10 m. The third response pattern consists of fairly continuous resistivity responses generally in the range 160 – 650 Ohm-m. With the exception of 84 – 96 m, this pattern extends throughout the traverse occurring between the shallow low resistivity pattern and deeper high resistivity responses described above. The pattern appears at the surface from before 10 m to 40 m, between 62 m and 78 m, and at 116 – 135 m. At locations 88 – 96 m and 125 – 135 m, this pattern extends to depths in excess of 10 m below the surface dividing the basal high resistivity response into segments. Subsurface conductivity response ranges from 6 – 23 mS along Tr. 1 (Figure 2) and presents as a rapidly oscillating response with a generally increasing trend from west to east. The highest conductivity (18 – 23 mS) occurs at approximately 90 – 110 m and is roughly coincident with the deep intermediate resistivity response which extends from the top to the base of the inverted 2D resistivity structure for this traverse. At 120 m, conductivity falls off very rapidly in a region coincident with another deep intermediate resistivity section in the inverted resistivity structure.

Figure 3 is a composite image of the inverted 2D resistivity section along Tr. 2 and the corresponding conductivity profile. Low resistivity response pattern (generally less than 150 Ohm-m) occur at shallow depths at 14 – 32 m, 36 – 46 m, 49 – 61 m and from 64 m till the northern end of the section. This pattern is restricted to a depth of less than 3 m below the surface with the exception of the most northerly response which extends to a depth of 7 m. The pattern at 14 – 32 m, apparently sits within a trough at the top of higher resistivity responses below. At depths below 4 m, high resistivity responses (> 1000 Ohm-m) dominate. This pattern is fairly continuous and homogeneous. It terminates at approximately 60 m along the traverse with a vertical edge indicative of the presence of a fracture. A third response pattern with intermediate resistivities in the range 160 – 650 Ohm-m separates the high resistivity response pattern from the lower resistivity pattern above. This pattern is poorly developed on this traverse. Traverse 2 presents with the smallest variation in subsurface conductivity; 6 – 10 mS. This may relate to the relatively monotonous, continuous and flat surfaced high resistivity response at shallow depth for most of the traverse. The highest conductivity values on this traverse (10 mS) occur in the northern extreme and appear to coincide with the deep weathering section north of the imaged edge of the high resistivity structure at depth (at 60 m).

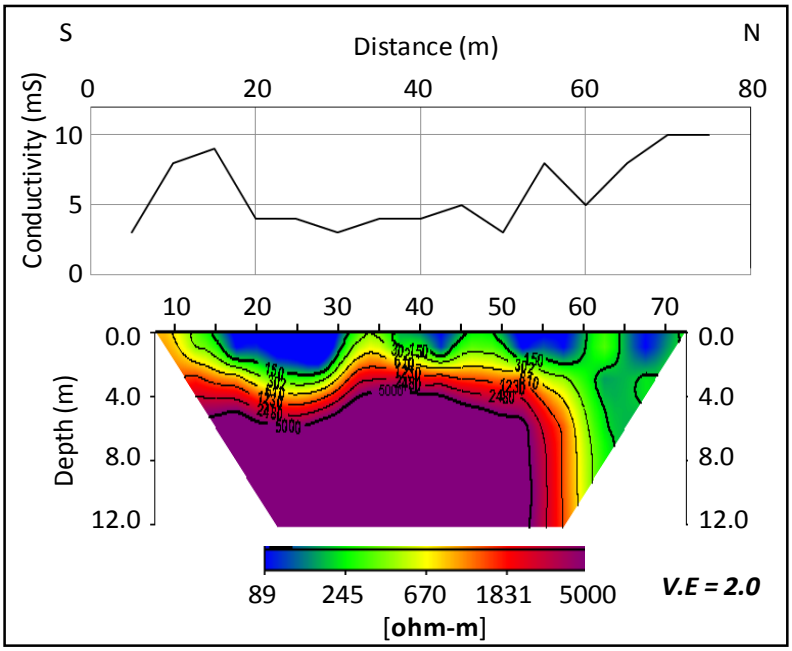

Figure. 3: Composite plot of inverted 2D subsurface resistivity structure (bottom) and ground conductivity at 10 m coil separation (top) along traverse 2. Overburden thickness is low with the exception of the northern end where the low resistivity bedrock response terminates in a near vertical scarp. (Vertical exaggeration in the 2D subsurface resistivity structure ≈ 2.0)

Figure 4 is the inverted 2D resistivity structure along Tr. 3. Low resistivity responses occur at shallow

depth (< 4 m) in the southern (10 – 32 m) and northern (60 – 73 m) extremes of the traverse. Between positions 25 – 32 m, this pattern extends to the base of the section (~ 12 m). High resistivity response patterns dominate at depths below 2 m from location 35 m to the northern end of the traverse. At 53 – 58 m, this pattern appears to reach to the surface. Intermediate resistivity patterns occur in southern end of the traverse at depths below 4 m and as a drape around the southern and upper limits of the high resistivity response to the north.

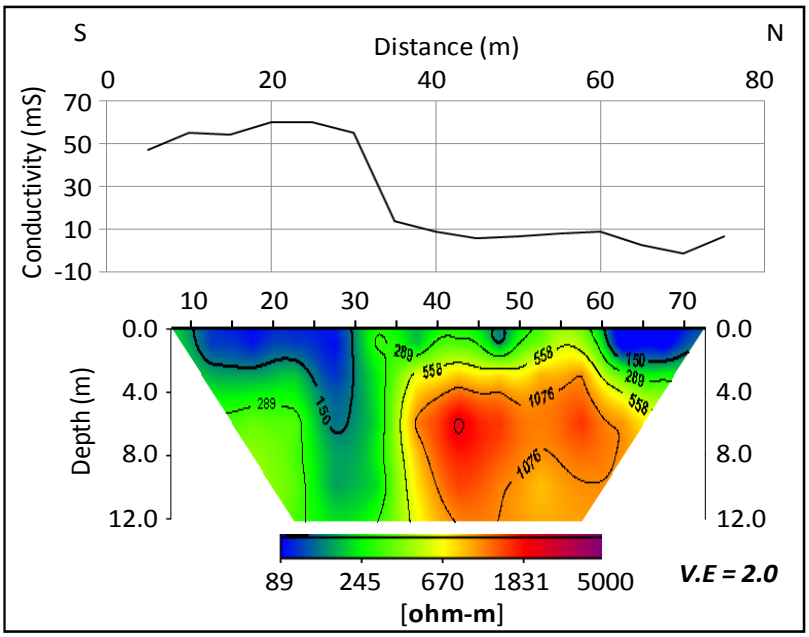

Figure. 4: Composite plot of inverted 2D subsurface resistivity structure (bottom) and ground conductivity at 10 m coil separation (top) along traverse 3. Deep weathering occurs in the southern end of the traverses and is possibly associated with a conductive fracture at position 23 – 31 m. (Vertical exaggeration in the 2D subsurface resistivity structure ≈ 2.0)

The largest variation in subsurface conductivity occurs along traverse 3; 0 – 60 mS. In the southern end of the traverse, from position 0 – 30 m, conductivity values are generally above 50 mS. Thereafter, conductivity drops off rapidly at position 35 m and maintains a trend generally below 10 mS all through to the northern end of the traverse. The rapid drop-off in conductivity values at 35 m is coincident with the edge of the high resistivity response imaged in the inverted 2D resistivity structure along the traverse. High conductivity along the traverse therefore coincide with low resistivity deep weathering/fracture sections in the bedrock while low conductivity relates to high resistivity fresh bedrock rise.

The low resistivity response pattern (generally < 150 Ohm-m) which occurs at the surface and rarely extends beyond 4 m depth was interpreted as the humus-rich topsoil which can be visually observed on the ground surface at the survey site. This topsoil appears well drained. The continuous high resistivity response (> 1000 Ohm-m) occurring at depth was interpreted to represent the un-weathered bedrock rock at the survey site. The intermediate resistivity response pattern was interpreted as representing either the zone of active weathering separating the topsoil from the un-weathered bedrock or fractured sections in the fresh bedrock depending on the geometric relationship of the patterns with other responses.

5. Discussions

Figure 5 is a composite fence diagram of the 2D subsurface resistivity structures presented earlier. Refer to figure 2 for actual spatial relationships and dimensions.

Three subsurface layers are delineated at the study location; [1] the shallow surficial humus-rich topsoil with resistivities generally below 150 Ohm-m, [2] the weathered bedrock with resistivities in the range 200 – 650 Ohm-m, and [3] the fresh bedrock with resistivities generally above 1000 Ohm-m. The topsoil and weathered bedrock form the overburden at the site. Overburden development is generally thin, not exceeding in most places 4 m. The exceptions are in the extreme northeast were the bedrock terminates in a near vertical interface, the southwest and the southeast and along the southern face of the survey site between 90 m and 100 m on traverse 1. The deep weathering section at 90 – 100 m possibly represents a fracture plane segmenting the fresh bedrock at this location. Deep weathering sections possibly conduct groundwater at the site. Specifically, the sections at 90 – 100 m along traverse 1 and at 0 – 30 m along traverse 3 present with relatively high conductivity (> 20 mS) values. In contrast, the deep overburden section at 0 – 35 m along traverse 1 and that in the northern extreme of traverse 2 present with much lower conductivities (< 15 mS). These possibly represent dryer conduits. Fresh bedrock occurrence is shallow and presents with a highly rugose topography. The lateral limits of the fresh bedrock are generally near-vertical while the summits are frequently associated with trough-like depressions. The surficial

topsoil frequently sits within these troughs in the apexes of the fresh bedrock expression. The fresh bedrock is severally segmented into blocks by the deep weathering sections which represent the overburden. It has been suggested that this association of near-vertical fresh bedrock scarps with proximal apixial troughs is characteristic of fault induced segmentation of the fresh bedrock (Aminu, 2015b).

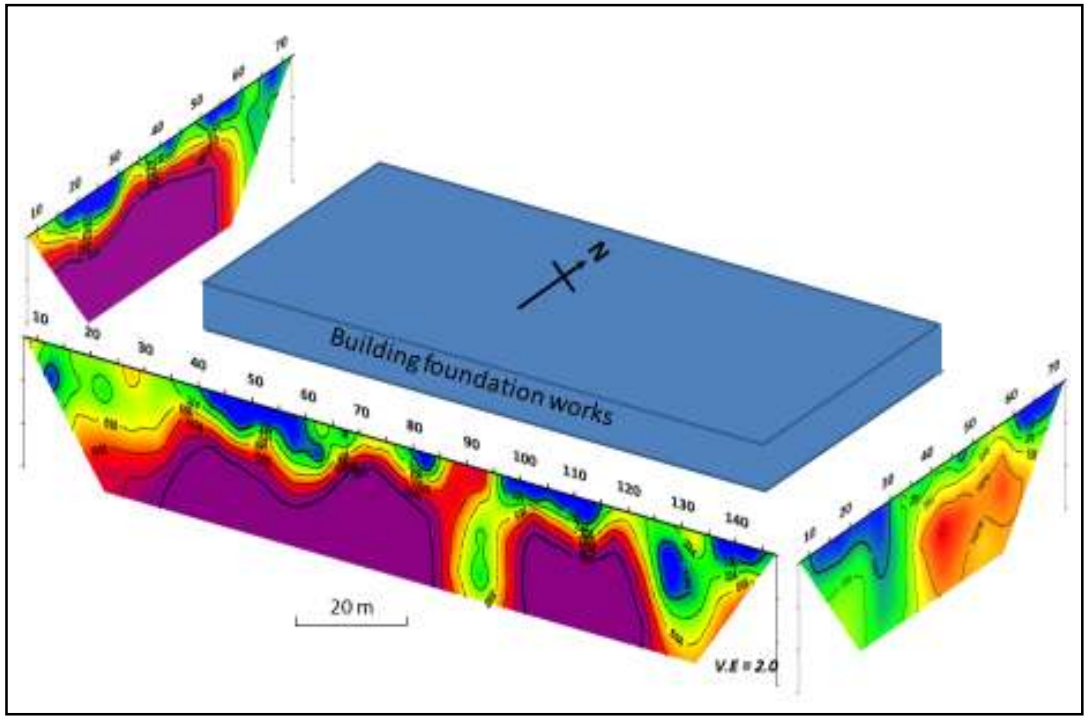

Figure. 5: Composite fence plot of all three traverses (viewing approximately from southeast). Overburden thickness is generally thin with the exception of the south-western and south-eastern fringes of the study area and vertical fracture positions segmenting the bedrock. Deep weathering sections in the southeast and the southern face of the study area likely serve to conduit groundwater through the site. (Refer to figure 1 for actual spatial separation between traverse).

Although bedrock topography is highly undulating, the thin overburden development over most of the site and the relatively low aperture width of the deep weathering section at 90 – 100 m along traverse 1 may be expected to pose minimal threat to civil works project. Sections which could prove problematic for construction works at the site lie principally in a broad region (position 5 - 35 m) in the southwest extreme (figure 5 and 6), where depth to bedrock decreases rapidly from less than 3 m at position 40 m along traverse 1 to beyond 7 m at position 10 m. This increase in thickness of the overburden could result in cantilever-style settling of sections of the building which may extend to the region. It therefore would be advisable that the bedrock topography provided by this study be considered in providing precautionary measures against building failure.

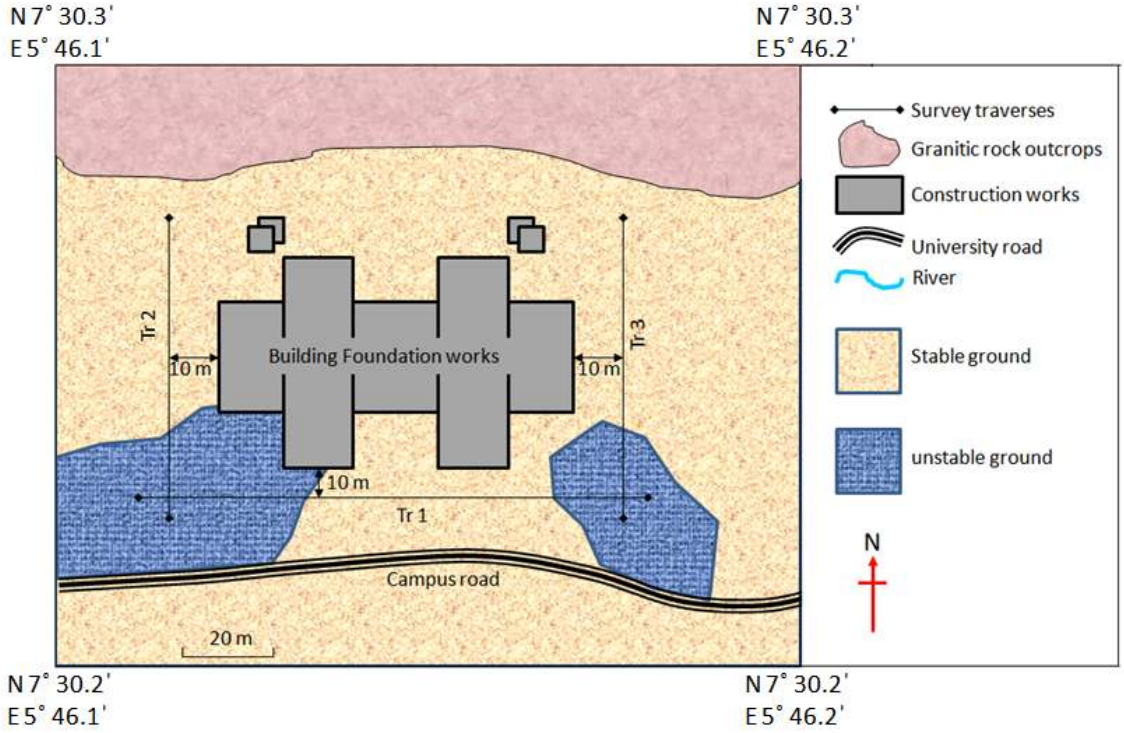

Figure. 6: Conceptual model indicating stable and potentially unstable subsurface material at the survey site. Unstable sections could pose threats to construction works.

6. CONCLUSIONS

A combination of 2D electrical resistivity imaging and electromagnetic ground conductivity surveying have been used to characterize the subsurface geological disposition at the site of an on-going civil-works construction project at Adekunle Ajasin University campus, Akungba-Akoko, south-western Nigeria. The goal was to identify subsurface geological features with potential to pose engineering threats to the on-going civil-works project. The results showed that depth to fresh bedrock is generally shallow and bedrock topography is highly rugose with occasional deep weathering sections. Multiple deep weathering sections and possibly fracture paths segment the bedrock into vertical scarp-faced blocks that serve as pathways for the conduction of groundwater through the site. The low aperture of the gaps between individual adjacent bedrock blocks and the low overburden thickness likely preclude the existences of major threats to the ongoing project. Proper foundation construction can easily span the indicated gaps and cantilever-type differential settling is unlikely. The possible threat occurs only in the board region in the southwest end of the sites where overburden thickness increases considerably and is indicated to consist of fairly low resistivity water saturated fills. In this region considerable differential settling can pose significant threat to the project. It would therefore be necessary for anticipatory precaution be taken to mitigate possible challenges.

ACKNOWLEDGEMENTS

I am grateful to Abdulateef Oladele, Olagide Jimoh and Oduanyo Ogele, all formerly of the Department of Earth Sciences, Adekunle Ajasin University, Akungba-Akoko, Nigeria, for assistance in data collection. I also acknowledge the anonymous reviewer(s) who's comments have made the manuscript more readable.

REFERENCES

Aminu, M. B., 2015a. Electrical Resistivity Imaging of a Thin Clayey Aquitard Developed on Basement Rocks in Parts of Adekunle Ajasin University Campus, Akungba-Akoko, South-western Nigeria. Environmental Research, Engineering and Management, 71(1), 47 – 55.

Aminu, M. B., 2015b. Geo-electric Investigation of the Cause of Structural Failure Indices on a Set of Administrative Blocks. Journal of Applied Geology and Geophysics, 3(4), 1-10.

Aminu, M. B., Akande, T. M., and Ishola, A. O., 2014. 2D Geoelectric Imaging of the Uneme-Nekhua Fracture Zone. International Journal of Geophysics, http://dx.doi.org/10.1155/2014/842812

Anderson, N. L., 2006. Selection of Appropriate Geophysical Techniques: A Generalized Protocol Based on Engineering Objectives and Site Characteristics. Proc., 2006 Highway NDE Conference, 2006, pp. 29–47. http://2006geophysics.mst.edu/.

Bufford, K. M., Atekwana, E. A., and Abdelsalam, M. G., 2012. Geometry and faults tectonic activity of the Okavango Rift Zone, Botswana: evidence from magnetotelluric and electrical resistivity

tomography imaging. Journal of African Earth Sciences, 65, 61–71.

Chávez, R. E., Cifuentes-Nava, G., Tejero, A., Hernández-Quintero, J. E., and Vargas, D., 2014. Special 3D electric resistivity tomography (ERT) array applied to detect buried fractures on urban areas: San Antonio Tecómitl, Milpa Alta, México. Geofísica Internacional 53(4), 425-434

Cosenza, P., Marmet, E., Rejiba, F., Cui, Y. J., Tabbagh, A., and Charlery, Y., 2006. Correlations between geotechnical and electrical data: A case study at Garchy in France, Journal of Applied Geophysics, 60(3), 2006, 165–178

El-Qady, G., Hafez, M., Abdalla, M. A., and Ushijima, K., 2005. Imaging subsurface cavities using geoelectric tomography and ground penetrating radar, Journal of Cave and Karst Studies, 67(3), 174–181.

Frid, V., Liskevich, G., Doudkinski, D., and Korostishevsky, N., 2007. Evaluation of landfill disposal boundary by means of electrical resistivity imaging. Environmental Geology, 53(7), 1503-1508.

Lines, J. P., Bernardes, S., He, J., Zhang, S., Bacchus, S. T., Madden, M., and Jordan, T., 2012. Preferential Groundwater Flow Pathways and Hydroperiod Alterations Indicated by Geo-rectified Lineaments and Sinkholes at Proposed Karst Nuclear Power Plant and Mine Sites. Journal of Sustainable Development, 5(12), 78-116.

Loke, M. H., 2000. Electrical imaging surveys for environmental and engineering studies: a practical guide to 2-D and 3-D surveys p. 61. http://www.heritagegeophysics.com/images/lokenote.pdf.

Mohamed, N. E., Brasse, H., Abdelgalil1, M. Y. and Kheiralla, K. M., 2012 Geoelectric and VLF electromagnetic survey on complex aquifer structures, Central Sudan. Comunicações Geológicas 99(2): 95-100.

Moustafa, S. S. R., Ibrahim, E. H., Elawadi, E., Metwaly, M. and Al Agami, N., 2012 Seismic refraction and resistivity imaging for assessment of groundwater seepage under a Dam site, Southwest of Saudi Arabia. International Journal of the Physical Sciences 7(48): 6230-6239.

Rahaman, M. A., 1989. Review of the Basement Geology of South-Western Nigeria, in: C. A. Kogbe (Ed), Geology of Nigeria, Nigeria: Rock View Limited) 39-56.

Rizzo, E., Colella, A., Lapenna, V., and Piscitelli, S., 2004. High-resolution images of the fault-controlled High Agri-Valley basin (Southern Italy) with deep and shallow electrical resistivity tomographies. Physical Chemistry of the Earth, 29 (4), 321–327.

Robineau, B., Join, J. L., Beauvais, A., Parisot, J-C., and Savin, C., 2007. Geoelectrical imaging of a thick regolith developed on ultramafic rocks: groundwater influence. Australian Journal of Earth Sciences, 54(5), 773-781.

Soupios, P. M., Georgakopoulos. P., Papadopoulos, N., Saltas, V., Andreadakis, A., Vallianatos, F., Sarris, A., and Makris, J. P., 2007. Use of engineering geophysics to investigate a site for a building foundation, Journal of Geophysics and Engineering, 4(1), 2007, 94–103.

Yassin, R. R., Muhammad, R. F., Taib, S. H., and Al-Kouri, O., 2014. Application of ERT and Aerial Photographs Techniques to Identify the Consequences of Sinkholes Hazards in Constructing Housing Complexes Sites over Karstic Carbonate Bedrock in Perak, Peninsular Malaysia. Journal of Geography and Geology, 6(3), 55-89.

Yi, M. J., and Kim, J. H., 1998. Enhancing the resolving power of the least squares inversion with Active Constraint Balancing: SEG Expanded Abstracts, 68 Annual Meeting, New Orleans, 485-488.

Zume, J. T., Tarhule, A., and Cristenson, S., 2006. Subsurface imaging of an abandoned solid waste landfill site in Norman, Oklahoma, Ground Water Monitoring and Remediation, 25(2), 2006, 62-69.